Available online at www.sciencedirect.com
ScienceDirect
Journal of Physics and Chemistry of Solids 68 (2007) 645–649
JOURNAL OF PHYSICS AND CHEMISTRY OF SOLIDS
www.elsevier.com/locate/jpcs

# Production of Sr-deficient bismuth tantalates from microwave–hydrothermal derived precursors: Structural and dielectric properties

Anderson Dias[a,*], Roberto L. Moreira[b]

[a]Departamento de Química, Universidade Federal de Ouro Preto, Campus Morro do Cruzeiro, 35400-000 Ouro Preto-MG, Brazil
[b]Departamento de Física, ICEx, UFMG, C.P. 702, Belo Horizonte-MG 30123-970, Brazil

Received 5 November 2006; received in revised form 3 February 2007; accepted 6 February 2007

**Abstract**

Strontium bismuth tantalates were produced for the first time from microwave–hydrothermal precursors at 200 °C, for 2 h. Structural and dielectric properties were investigated by X-ray diffraction and complex impedance spectroscopy. A high ferroelectric–paraelectric transition temperature of 375 °C ($T_c$) was observed, together with two different dielectric regimes for the ac electrical conductivity below $T_c$. The activation energies were calculated as 0.155 and 0.531 eV, and are related to conduction by oxygen vacancies. It was concluded that the low activation energies showed by these materials could contribute to their fatigue-free nature.


*Keywords:* A. Ceramics; B. Chemical synthesis; D. Dielectric properties

## 1. Introduction

Strontium bismuth tantalate ($SrBi_2Ta_2O_9$) has been extensively studied in the last decade because of its ferroelectric and structural flexibilities suitable for ferroelectric integrated devices [1]. Its structure consists of alternating layers of $(Bi_2O_2)^{+2}$ and pseudoperovskite $(SrTa_2O_7)^{-2}$ blocks in a global orthorhombic symmetry ($A2_1am$ space-group). The $Bi_2O_2$ layers and $TaO_6$ octahedra are considerably distorted and the atomic displacements along the *a*-axis give rise to a spontaneous polarization along this direction [1]. A large number of studies have been reported mainly on the formation of films by different processes [2]. However, the literature regarding the preparation of ceramics is limited to conventional solid-state method and a few non-conventional routes [3].

Nowadays, there is a considerable interest in evaluating new methods for the synthesis of functional electroceramics in order to achieve better control over physical and chemical properties [4]. The hydrothermal synthesis route presents the highest technological potential to obtain electroceramics [5–7] due to its low-temperature and environmentally friendly processing conditions, which allows the production of ultrafine, crystalline powders in a single step. A recent innovation in the hydrothermal process is the introduction of microwaves into the reaction vessels, which enhances the kinetics of crystallization [8]. In this paper, Sr-deficient bismuth tantalates (SBT) were produced for the first time from microwave–hydrothermal derived precursors. For these ceramics, it is well known that *A*-site-deficient materials exhibit enhanced ferroelectric properties. The structural and dielectric properties are studied and, in addition to the ferroeletric–paraelectric phase transition, it was observed two conduction regimes in the dielectric constant and ac electrical conductivity attributed to oxygen vacancies.

## 2. Experimental

$SrCl_2.6H_2O$ (>99%), BiOCl (99.99%), $TaCl_5$ (99.9%) and NaOH (99.99%) (Fluka Chemie AG and Aldrich Chemical Company) were used as starting chemicals for

*Corresponding author. Tel.: +55 31 3559 1707.
*E-mail address:* anderson_dias@iceb.ufop.br (A. Dias).

0022-3697/$ - see front matter © 2007 Elsevier Ltd. All rights reserved.
doi:10.1016/j.jpcs.2007.02.006

SBT. The cationic molar ratio employed was $Sr/Bi = 0.4$, aiming to the production of a Sr-deficient, Bi-rich SBT phase. Each reagent was previously dissolved in deionized water (18.2 MΩ cm) and mixed under vigorous stirring. NaOH was then added to the aqueous solution in order to precipitate the oxyhydroxides at $pH > 13$. Microwave–hydrothermal processing was performed using a Milestone MLS-1200 MEGA microwave digestion system (2.45 GHz). The system was programmed to work at 1000 W, for 10 min, up to the processing temperature (200 °C) and maintained at 400 W, for 2 h. The resulting precursors were repeatedly washed with hot deionized water in order to remove any Na ions present (NaCl) and dried at 80 °C. Besides, to detect the presence of sodium in the powders after microwave–hydrothermal synthesis, different characterization methods like energy dispersive X-ray (EDX) spectroscopy and atomic absorption spectrometry (AAS) were used. In all cases, sodium ions were not detected, indicating that the amount of sodium ions, if present, is below the maximum detection limits of the used techniques. Chemical analysis (AAS-Perkin Elmer 5000) indicated that a Sr-deficient precursor was obtained with final composition $Sr_{0.85}Bi_{2.1}Ta_2O_9$. Heat treatments occurred in conventional furnaces (air atmosphere), in temperatures ranging from 600 to 1000 °C, for 30 min, aiming to study the structural evolution under heating of the microwave–hydrothermal derived powders.

Structural characterization was carried out in a Philips PW1710 diffractometer with graphite monochromated Cu$K\alpha$ radiation, Ni filter and $3-100°2\theta$ ($0.02°2\theta$ step/s). Scanning and transmission electron microscopies (JEOL 5410 and Philips CM200) were employed to study the morphological features of the microwave–hydrothermal precursors. The results showed particles ranging from 20 (200 °C) to 120 nm (1000°C) in size and with nearly cubic morphology. Adsorption nitrogen analysis (Quantachrome) showed corresponding specific surface areas of about $6-34\ m^2/g$ in good agreement with the results from microscopy. The powders were uniaxially pressed at 110 MPa into cylindrical disks of 15 mm diameter and 5 mm height. Sintering occurred at 1100 °C for 4 h in a closed alumina crucible to prevent Bi volatilization. Dielectric characterization was carried out in a HP 4192A impedance analyzer. Gold electrodes were fabricated by sputtering on both sides of the sintered sample and the measurements were done in the frequency range 10 Hz–13 MHz, from room temperature up to 500 °C. The temperature-increasing rate was controlled at 2 °C/min.

## 3. Results and discussion

SBT belongs to a family of layered-perovskites structurally described by Aurivillius and recently recalculated by Rae et al. [9]. Fig. 1 presents the X-ray powder diffraction (XRD) data for the microwave–hydrothermal powders (MHP in Fig. 1a), as well as the patterns for the samples heated at 600, 700, 800, 1000 and 1100 °C (Figs. 1b–f). The

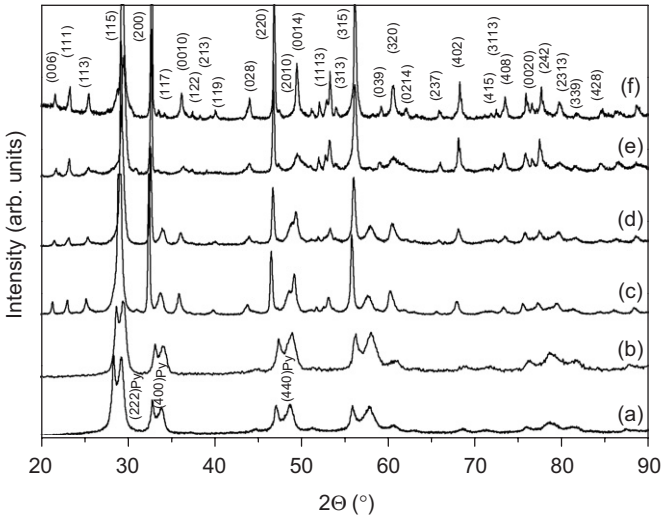


Fig. 1. XRD patterns for the SBT powders. (a) MHP and samples heated at (b) 600 °C, (c) 700 °C, (d) 800 °C, (e) 1000 °C, and (f) 1100 °C.

phases found after microwave processing appeared to be a mixture of the SBT phase (ICDD #49-0609) and another phase with cubic structure ($Fd\bar{3}m$). There are no evidences of any Sr–Bi-oxide or Bi–Ta-oxide phases. Also, it was observed a shift in $2\theta$ for the main reflections of the SBT compound—(1 1 5), (2 0 0), (2 2 0), (3 2 0), (4 0 2), and (4 0 8), indicating a structural variation in the unit cell. This shift could be related to the stoichiometric deviation verified by chemical analysis after processing towards a Sr-deficient SBT phase.

If the samples are not stoichiometric, Bi cations could occupy the Sr sites within the perovskite sublattice [3,10,11]. Boyle et al. [12] present a theory in which the SBT structure appears to be preceded by the formation of an "intermediate phase". It is well-known that substitution of trivalent Bi ions for divalent Sr ions generate cation vacancies [11]. As it can be seen in Figs. 1a and b, the diffraction patterns present broad diffraction peaks at 29.3°, 34°, 48.8° and 57.8°, which is attributed to an intermediate cubic phase for SBT formation [12]. As the temperature is raised, the diffraction patterns changed significantly (Fig. 1c–f). For the sample heated at 700 °C (Fig. 1c), several structural modifications can be observed: the amount of SBT phase increases substantially, but the pyrochlore phase is also present. Above 800 °C, the SBT phase (Fig. 1d–f) can be easily visualized. Fig. 1f shows the XRD pattern for the sample heated at 1100 °C, where the orthorhombic phase is observed.

The possibility of forming cubic $Fd\bar{3}m$ structure within the SBT system depends on the ability to create a cation-defective structure, which may consider the various valence states of the cations. In this respect, Ehlert et al. [13] reported a defect pyrochlore-type structure for Bi–Ta oxides, while Lu et al. [14] identified a new pyrochlore phase in the Sr–Bi–Ta–Ti–O system. The structure described by Ehlert et al. ($RbBi_2Ta_5O_{16}$, ICDD #43-0291) [13] can be considered as a possible match for the

diffraction peaks observed in the MHP. Rodriguez et al. [15] calculated the XRD patterns for a similar cation-defect structure having a $Fd\bar{3}m$ symmetry, with the Ta cations residing within an oxygen octahedra and the Bi cations sitting between the Ta–O octahedra. Strontium was incorporated into the lattice by assuming that it behaves similarly to Rb cation, but with the possibility of site mixing with Bi. Finally, an estimated stoichiometry for this pyrochlore (or intermediate phase) was proposed by Rodriguez et al. as $Sr_{0.2}(Sr_{0.5}Bi_{0.7})Ta_2O_{6.75}$, which is deleterious for SBT formation due to its strong Bi-deficient character [15]. In the present work, it was verified that an "intermediate phase" was produced during microwave–hydrothermal processing, which is instable under heating. Conversely to the results of Rodriguez et al. [15] and Ami et al. [16], the pyrochlore phase found in the present work was converted to the orthorhombic phase above 800 °C, as it can be seen in Fig. 1.

Microwave–hydrothermal derived SBT ceramics were sintered at 1100 °C and its dielectric properties were investigated in detail. XRD results for these samples were obtained and compared to those observed for the only-heated sample of Fig. 1f. Almost identical patterns were observed for both samples (calcined and sintered SBT materials). Energy-dispersive spectrometry analysis was not able to detect any Bi-loss by volatilization in the samples. Fig. 2 presents the dielectric constant ($\varepsilon'$) as a function of temperature and frequency for the ceramic sintered at 1100 °C. As a general trend, $\varepsilon'$ increases for increasing temperature up to the ferroelectric–paraelectric phase transition. For the samples studied in the present work, the Curie temperatures ($T_c$) were found at 375 °C, which agree well with those currently found in the literature for Sr-deficient SBT [3,10,11,17]. In these compounds, the spontaneous polarization is two times larger than that of stoichiometric SBT, and the ferroelectric phase transition ($T_c$) shifts to around 400 °C from 330 °C.

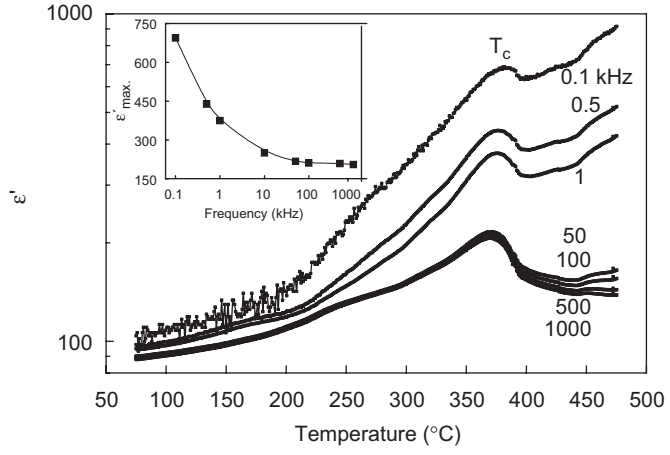


Fig. 2. Dielectric constant ($\varepsilon'$) as a function of temperature and frequency for the SBT ceramic. $T_c$ is the temperature of the ferroelectric–paraelectric phase transition. Inset: $\varepsilon'_{max}$ (observed at $T_c$) versus frequency.

Miura and Panda et al. [18,19] reported that the excess of Bi leads to the substitution of trivalent Bi ions for divalent Sr ions, enhancing the structural distortion in $TaO_6$ octahedra and the spontaneous polarization. Fig. 2 shows that $T_c$ is slightly round-shape and also independent on the measuring frequency. The dielectric constant decreased with increasing frequency, from 677 at 100 Hz to 206 at 1 MHz (see inset in Fig. 2). This behavior is linked to the ionic conductivity of the sample and will be shown and discussed later.

Besides the ferroelectric–paraelectric phase transition, Fig. 2 also shows that the temperature dependence of the dielectric constant presents two different temperature regimes: $\varepsilon'$ increases slightly below temperatures around 210−240 °C, increasing substantially above this temperature and below $T_c$. According to Onodera et al. [17], this behavior could be related to thermally stimulated space charges (TSSC). Jimenez et al. [20] studied the temperature dependence of remnant polarization of Sr-deficient Bi-rich SBT ceramics deduced from measurements of switching currents and pulsed hysteresis loops. The authors verified a change in the slope of polarization versus temperature curves around 200 °C and attributed this behavior to a phase transition, also claimed by Onodera et al. in another paper [11]. Jimenez et al. [20] pointed out that the rapid decrease in the remnant polarization with temperature up to 200 °C is of practical interest, considering the application of these materials as non-volatile ferroelectric memories. The results on $\varepsilon'$ displayed in Fig. 2 showed an indication of a change in this property for increasing temperature and frequency.

Fig. 3 presents the electrical conductivity of the SBT ceramic as a function of temperature and frequency, where the two conduction regimes mentioned above can be clearly seen. First, a high ionic conduction with relatively free charge carriers is observed, reflected in the increasing conductivity with frequency and temperature. These charges are also responsible for the dielectric constant dispersion seen in Fig. 2. The phase transition at 375 °C appears like a round peak in the electrical conductivity, which varies as a function of frequency: $\sigma \approx 5 \times 10^{-5}\,\Omega^{-1}\,cm^{-1}$ at 100 kHz, and $\sigma \approx 2 \times 10^{-4}\,\Omega^{-1}\,cm^{-1}$ at 1 MHz ($T = 375$ °C). The temperature where the second regime starts (denoted $T^*$) can be inferred from the change in slope in conductivity plot (inset in Fig. 3), where it can be seen that $T^*$ increases with frequency. This result means that a structural transition is not responsible for this behavior. According to Tanaka et al. [17], both pulse switching charge and non-switching response charge showed "anomalous" thermal behaviors in the temperature range 150−250 °C. The authors claim that the major part of the effect is due to the field-induced charge without ferroelectric-polarization switching. For the samples studied in the present work, the variation in $T^*$ with frequency is probably due to a stoichiometric deviation observed after microwave processing. Thus, oxygen vacancies or Bi ions with oxidation state equal to +2 could generate space

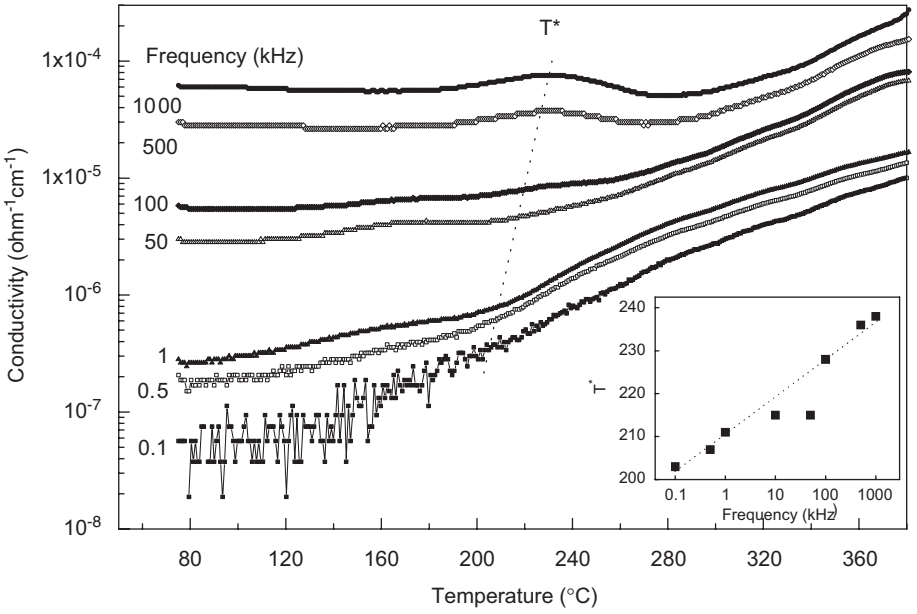


Fig. 3. The ac electrical conductivity as a function of temperature and frequency for the sintered SBT. $T^*$ is the temperature in which a change in the conduction regime was observed. Inset: $T^*$ versus frequency.

charges within the ceramic, producing the observed behavior in $\varepsilon'$ and $\sigma$.

In order to understand the conduction process in the Sr-deficient SBT ceramics obtained from microwave–hydrothermal precursors, the temperature dependence of the ac conductivity at various frequencies was evaluated. Fig. 4 shows the Arrhenius plot of the electrical conductivity of the sintered SBT ceramic at 1 kHz. As it can be seen, two different regions (or slopes) are clearly identified. These two slopes mean different behaviors in the total conductivity due to TSSC. In each region, the electrical conductivity can be described by

$$\sigma T = (ne^2 l^2 v_0/\kappa)\exp^{-E/\kappa T}, \quad (1)$$

where $n$ is the density of charge carriers, e is the electron charge, $l$ is the distance between the trap sites, $v_0$ is the characteristic frequency, $\kappa$ is the Boltzmann constant, $T$ is the absolute temperature, and $E$ is the activation energy of the TSSC process. The pre-exponential factor $(ne^2 l^2 v_0/\kappa)$ reflects the carrier concentration. The activation energies before and after $T^*$ were obtained from the linear portions of the plots of log $(\sigma T)$ versus $10^4/T$, as showed in Fig. 4. The results showed values of 0.155 and 0.531 eV for the conduction process, below and above 210 °C ($T^*$), respectively.

It is well known that oxygen vacancies are the most mobile charges in oxide ferroelectrics [21]. This should also be the case for SBT material, even though two different processes are present here. Indeed, due to the structural anisotropy of the material, mainly because the oxygen octahedra of the pseudo-perovskite blocks are disconnected by the $Bi_2O_2$ layers, the macroscopic conduction by oxygen vacancies is likely divided up in two steps: inner motif (into the blocks) movements, and jumps between

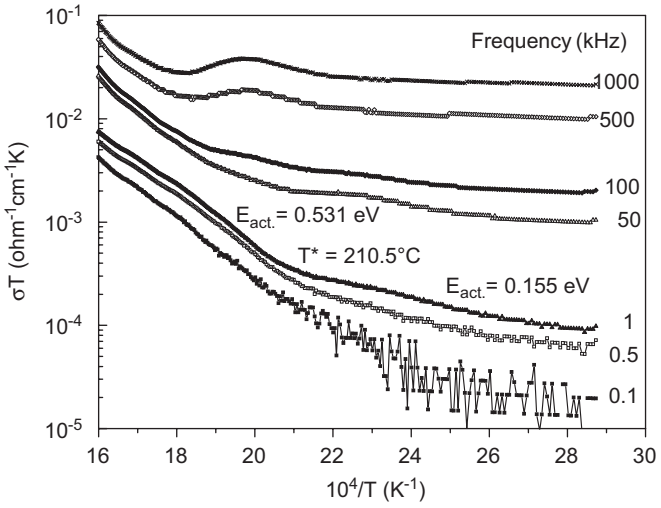


Fig. 4. Arrhenius plot for the electrical conductivity of SBT ceramics sintered at 1100 °C/4 h as a function of frequency. The activation energies were obtained from the slopes of the straight lines in each region (for 1 kHz, $T^*$ is also indicated).

motifs through the $Bi_2O_2$ layers. At lower temperatures (below $T^*$) the oxygen vacancies only have energy to exchange positions with neighbor ions, which requires low activation energies (0.155 eV). At higher temperatures ($T^* < T < T_c$), the vacancies would have enough energy to jump over larger distances, with a higher activation energy (0.531 eV), so that this would become the dominating conduction mechanism into the material.

Now, we could wonder what is the origin of the oxygen vacancies in our system. It is worthy noticing that Shimakawa et al. [22] and Miyayama and Noguchi [23] studied the crystal structures, polarization properties, and

oxygen-vacancy distribution in Sr-deficient and stoichiometric SBT modified by rare earth doping. The authors observed that oxygen vacancies are present in the $Bi_2O_2$ layers to compensate the charge difference between the different ions: $Sr^{+2}$ and trivalent rare-earth in doped samples, and $Sr^{+2}$ and $Bi^{+3}$ in Sr-deficient SBT materials. In this work, the microwave–hydrothermal process was employed to produce suitable precursors for Sr-deficient, Bi-rich SBT ceramics, decreasing the sintering temperature and allowing the observation of the oxygen motion. For these materials, the fatigue-free nature is attributed to the fact that the oxygen vacancies can easily move.

## 4. Conclusions

Microwave–hydrothermal processing was employed to produce SBT precursors for the first time. $Sr_{0.85}Bi_{2.1}Ta_2O_9$ ceramics were obtained together with a cubic phase, which transforms to the $A2_1am$ structure above 800 °C. This unexpected behavior for common pyrochlore phases is explained with basis on the formation of an intermediate cubic disordered structure with stoichiometry very close to the main phase. The ferroelectric–paraelectric transition was found to occur at 375 °C, which is in agreement with a Sr-deficient phase. Also, two conduction regimes below $T_c$ were observed in $\varepsilon'$ and $\sigma$, with a slight dependence on the measuring frequency, which are also an indication of stoichiometric deviation. The presence of vacancies and Bi ions mixed with Sr ions produces TSSC. The activation energies before and after the observed change in slope of the Arrhenius plot (210−240 °C) were determined as 0.155 and 0.531 eV, respectively. This report presents the first direct evidence of the space charges contributions in SBT, observed through impedance spectroscopy, notably in the dielectric constant.

## Acknowledgments

The authors acknowledge the financial support from the Brazilian agencies MCT/CNPq, FINEP and FAPEMIG.

## References

[1] R. Ramesh, S. Aggarwal, O. Auciello, Science and technology of ferroelectric films and heterostructures for non-volatile ferroelectric memories, Mater. Sci. Eng. R 32 (2001) 191–236.
[2] K. Kato, C. Zheng, J.M. Finder, S.K. Dey, Sol–gel route to ferroelectric layer-structured perovskite $SrBi_2Ta_2O_9$ and $SrBi_2Nb_2O_9$ thin films, J. Am. Ceram. Soc. 81 (1998) 1869–1875.
[3] K. Babooram, Z.-G. Ye, New soft chemical routes to ferroelectric $SrBi_2Ta_2O_9$, Chem. Mater. 18 (2006) 532.
[4] P. Vicenzini, Ceramics Today–Tomorrow's Ceramics, Elsevier, The Netherlands, 1991.
[5] A. Dias, R.M. Paniago, V.T.L. Buono, Influence of hydrothermal powder morphology on the sintered microstructure of MnZn ferrites, J. Mater. Chem. 7 (1997) 2441–2446.
[6] A. Dias, V.T.L. Buono, V.S.T. Ciminelli, R.L. Moreira, Hydrothermal synthesis and sintering of electroceramics, J. Eur. Ceram. Soc. 19 (1999) 1027–1031.
[7] A. Dias, V.T.L. Buono, V.S.T. Ciminelli, R.L. Moreira, Piezoelectric and relaxor materials synthesized by hydrothermal processing, J. Korean Phys. Soc. 32 (1998) S1159–S1162.
[8] A. Dias, V.S.T. Ciminelli, Electroceramic materials of tailored phase and morphology by hydrothermal technology, Chem. Mater. 15 (2003) 1344–1352.
[9] A.D. Rae, J.G. Thompson, R.L. Withers, Structure refinement of commensurately modulated bismuth strontium tantalate, $Bi_2SrTa_2O_9$, Acta Crystallogr. B 48 (1992) 418.
[10] A. Onodera, T. Kubo, K. Yoshio, S. Kojima, H. Yamashita, T. Takama, Crystal structure of high-temperature paraelectric phase in Bi-layered perovskite $SrBi_2Ta_2O_9$, Jpn. J. Appl. Phys. 39 (2000) 5711–5715.
[11] A. Onodera, K. Yoshio, C.C. Myint, S. Kojima, H. Yamashita, T. Takama, Thermal and structural studies of phase transitions in layered perovskite $SrBi_2Ta_2O_9$, Jpn. J. Appl. Phys. 38 (1999) 5683–5685.
[12] T.J. Boyle, C.D. Buchheit, M.A. Rodriguez, H.N. Al-Shareef, B.A. Hernandez, B. Scott, J.W. Ziller, Formation of $SrBi_2Ta_2O_9$. 1. Synthesis and characterization of a novel "sol–gel" solution for production of ferroelectric $SrBi_2Ta_2O_9$ thin films, J. Mater. Res. 11 (1996) 2274–2281.
[13] M.K. Ehlert, J.E. Greedan, M.A. Subramanian, Novel defect pyrochlores $ABi_2B_5O_{16}$ (A = Cs, Rb; B = Ta, Nb), J. Solid State Chem. 75 (1988) 188–196.
[14] C.H. Lu, B.K. Fang, C.Y. Wen, Structure identification and electrical properties of the new pyrochlore phase in the Sr–Bi–Ta–Ti–O system, Jpn. J. Appl. Phys. 39 (2000) 5573–5576.
[15] M.A. Rodriguez, T.J. Boyle, B.A. Hernandez, C.A. Buchheit, M.O. Eatough, Formation of $SrBi_2Ta_2O_9$: part II. Evidence of a bismuth-deficient pyrochlore phase, J. Mater. Res. 11 (1996) 2282–2287.
[16] T. Ami, K. Hironaka, C. Isobe, N. Nagel, M. Sugiyana, Y. Ikeda, K. Watanabe, A. Machida, K. Miura, M. Tanaka, Mater. Res. Soc. Symp. Proc. 415 (1996) 195.
[17] M. Tanaka, K. Hironaka, A. Onodera, Charge properties of Bi-rich strontium bismuth tantalate thin films, Jpn. J. Appl. Phys. 39 (2000) 5472–5475.
[18] K. Miura, T. Tanaka, Difference in the electronic structure of $SrBi_2Ta_2O_9$ and $SrBi_2Nb_2O_9$, Jpn. J. Appl. Phys. 37 (1998) 606–607.
[19] A.B. Panda, A. Pathak, M. Nandagoswami, P. Pramanik, Preparation and characterization of nanocrystalline $Sr_{1-x}Bi_{2-x}Ta_2O_9$ powders, Mater. Sci. Eng. B 97 (2003) 275.
[20] R. Jimenez, C. Alemany, M.L. Calzada, P. Tejedor, J. Mendiola, Temperature dependence of ferroelectric properties of SBT thin films, J. Eur. Ceram. Soc. 21 (2001) 1601–1604.
[21] I.W. Kim, C.W. Ahn, J.S. Kim, T.K. Song, J.S. Bae, B.C. Choi, J.H. Jeong, J.S. Lee, Low-frequency dielectric relaxation and ac conduction of $SrBi_2Ta_2O_9$ thin film grown by pulsed laser deposition, Appl. Phys. Lett. 80 (2002) 4006–4008.
[22] Y. Shimakawa, Y. Kubo, Y. Nakagawa, T. Kamiyama, H. Asano, F. Izumi, Crystal structures and ferroelectric properties of $SrBi_2Ta_2O_9$ and $Sr_{0.8}Bi_{2.2}Ta_2O_9$, Appl. Phys. Lett. 74 (1999) 1904–1906.
[23] M. Miyayama, Y. Noguchi, Polarization properties and oxygen-vacancy distribution of $SrBi_2Ta_2O_9$ ceramics modified by Ce and Pr, J. Eur. Ceram. Soc. 25 (2005) 2477–2482.